Dieter H. Szolar, MD • Fritz Kammerhuber, MD • Stefan Altziebler, MD • Manfred Tillich, MD
Eckehardt Breinl, MD • Richard Fotter, MD • Heribert H. Schreyer, MD

Multiphasic Helical CT of the Kidney: Increased Conspicuity for Detection and Characterization of Small (<3-cm) Renal Masses[1]

PURPOSE: To evaluate the potential of thin-section multiphasic helical computed tomography (CT) in the detection and characterization of small (<3.0-cm) renal masses.

MATERIALS AND METHODS: Identically collimated helical CT of the kidney was performed before and after administration of contrast material in 93 patients with small renal masses. Helical CT scans were obtained during the corticomedullary and nephrographic phases. Differences between attenuation of the lesion and that of the kidney were measured quantitatively. The presence of a mass or absence of disease was confirmed with clinical, imaging, and histologic findings.

RESULTS: The number of masses smaller than 3.0 cm detected on corticomedullary-phase scans ($n = 211$) was statistically significantly fewer than those on nephrographic-phase scans ($n = 295$) ($P < .01$). Mean differences in enhancement between the renal cortex and masses were 148 HU ± 54 and 137 HU ± 44 during the corticomedullary and nephrographic phases, respectively, and the difference in attenuation of the renal medulla and that of the masses was statistically significantly greater during the nephrographic phase ($P < .01$). False-positive results ($n = 9$) occurred only on corticomedullary-phase scans because of lack of enhancement of the renal medulla.

CONCLUSION: Nephrographic-phase scans enabled greater lesion detection and better characterization of small renal masses than corticomedullary-phase scans. Nephrographic-phase scans should be obtained when only monophasic scanning is used to detect small renal masses.

THE prognosis of renal cell carcinoma (RCC) depends on the size, stage, and grade of the tumor. Several studies have documented the increasing number of small RCCs (<3.0 cm) detected and the salutary effect of removal of these tumors on patient survival (1–5). Statistics compiled by the American Cancer Society (6) show that the 5-year survival rate for white Americans with RCC increased from 37% in the early 1960s to 56% in the early 1980s. This increase in detection of small renal lesions has been attributed to the increased use and widespread application of ultrasonography and conventional computed tomography (CT) rather than to an actual increase in the incidence of RCC (7,8).

The introduction of helical CT has created important advances in detection, characterization, and subsequent treatment of disease throughout the body (9–11). Helical CT has many advantages over conventional CT for the evaluation of renal disease. First, the elimination of respiratory misregistration ensures that the entire lesion is imaged and that the chance of identifying small enhancing lesions is maximized. Second, the acquisition of volumetric data during a single breath hold allows comparison of identical levels on scans obtained before and after administration of contrast material. Third, partial volume averaging is minimized because a section through the center of a lesion is assured with helical CT when overlapping sections are reconstructed. Thus, helical CT is the best technique for characterization of renal masses smaller than 3.0 cm, which are particularly difficult to characterize owing to their susceptibility to respiratory misregistration and partial volume effects.

Controversies exist, however, with regard to an optimal helical CT protocol for dedicated renal parenchymal imaging. While most investigators have emphasized the utility of images obtained during the corticomedullary phase of renal enhancement (12–15), only a few have performed helical CT of small renal masses during the nephrographic phase. To our knowledge, there is only one report of the use of helical CT for the assessment of renal masses during the two phases of renal enhancement (16). The series, however, is limited by a relatively small number of patients, the inclusion of analysis of only two solid masses, a marked temporal inhomogeneity in performing the nephrographic phase scanning, and a lack of quantitative evaluation.

The purpose of our study was to evaluate the potential of identically collimated, thin-section helical CT scans obtained before and during the corticomedullary and nephrographic phases of contrast material enhance-

Index terms: Computed tomography (CT), helical, 81.12115, 81.12119 • Computed tomography (CT), technology, 81.12112, 81.12115 • Kidney neoplasms, CT, 81.30 • Kidney neoplasms, diagnosis, 81.31, 81.32

Abbreviation: RCC = renal cell carcinoma.

Radiology 1997; 202:211–217

[1] From the Departments of Radiology (D.H.S., F.K., M.T., R.F., H.H.S.) and Urology (S.A., E.B.), Karl-Franzens Medical School and University Hospital, Auenbrugger-platz 9, 8036 Graz, Austria. From the 1996 RSNA scientific assembly. Received May 15, 1996; revision requested June 20; revision received July 30; accepted August 5. **Address reprint requests to** D.H.S.

See also the editorial by Urban (pp 22–23) in this issue.

ment in the detection and characterization of small (< 3.0-cm) renal masses in a representative study population.

MATERIALS AND METHODS

Study Population and Imaging Protocol

The study protocol was approved by and was in accordance with the recommendations of the human research committee of our institution. Written informed consent was obtained from all patients.

One hundred forty-three patients referred for small renal masses that had been suspected or detected with conventional CT, sonography, or excretory urography were consecutively examined with helical CT and considered for entry into the study. The study group initially consisted of 85 men and 58 women aged 23–85 years (mean, 57 years). Proof of individual masses was obtained on the basis of biopsy results, surgical findings, findings with other imaging modalities (primarily follow-up CT or sonography), and results of clinical follow-up. Nine patients had surgically verified masses (> 3 cm in diameter), and 11 had renal cysts or tumors (> 3 cm in diameter) of the kidney not treated with surgery (metastatic tumor to the kidney). Patients with inflammatory renal disease (abscess, $n = 1$; focal bacterial nephritis, $n = 2$), pseudotumors of the kidney (renal column, $n = 5$; renal dysmorphism, $n = 1$; unusual-shaped kidney, $n = 2$), renal infarction ($n = 1$), and adrenal gland masses ($n = 2$) were excluded from the study. Fourteen patients did not have a renal mass. The absence of disease was established at follow-up sonography or helical CT and at clinical follow-up that involved blood and urine sampling and occurred 3–9 months later. Two patients who could not tolerate breath hold or an adequate catheter size for injection of contrast material were excluded.

The remaining 93 patients (59 men and 34 women; aged 29–85 years; mean, 59 years) fulfilled the criteria for inclusion in the study protocol. Thirty-two patients with masses 3 cm or less in diameter underwent total ($n = 28$) or partial ($n = 4$) nephrectomy. Surgery was chosen as treatment (in consultation with referring urologists and patients) on the basis of the guidelines of Bosniak (7,8). Sixty-one patients did not require surgery, since they had renal cysts ($n = 59$) or tumors of the kidney (angiomyolipoma, $n = 2$). Confirmation of these individual lesions was based on the results of clinical follow-up, laboratory findings (blood and urine samples), or imaging follow-up (sonography or helical CT).

All studies were performed with a Somatom Plus 4 helical scanner (Siemens, Erlangen, Germany). All scans were obtained at 292 mA and 120 kV. The helical CT protocol for all patients consisted of volumetric data acquisition through the kidneys with 5-mm collimation, 7.5 mm/sec table feed, and 4-mm increments before and after intravenous administration of a contrast material bolus (50 seconds and 180 seconds). The scan time for one revolution of the x-ray tube was 0.75 seconds.

All scans (acquisition time, 18–24 seconds per scan) were obtained with the patient in full inspiration to optimize the reproducibility of starting levels. Unenhanced scans were obtained initially through the kidneys. An 18- or 20-gauge intravenous catheter (Angiocath; Becton-Dickinson, Franklin Lakes, NJ) was then placed in an antecubital vein and tested by rapidly infusing 10 mL of saline by hand. Subsequent to that step, 120 mL of the nonionic contrast material iopromide 300 (Ultravist; Schering Pharmaceuticals, Berlin, Germany) was infused at a rate of 2.5 mL/sec with a power injector (MCT Plus; Medrad, Pittsburgh, Pa). The second helical scan (corticomedullary phase) was started 50 seconds after the beginning of infusion and was followed by a repeat scan that was preprogrammed for the same collimation, table feed, and duration as was used in the previous two scans.

The third helical scan (nephrographic phase) began 169–194 seconds (mean, 180 seconds ± 5 [standard deviation]) after the beginning of injection of contrast material. Images were obtained with standard soft-tissue window and level settings (400 and 40 HU).

Image and Data Analysis

Image interpretation and measurement of attenuation for all scans were performed independently with a commercially available Sparc 10 CT and magnetic resonance workstation (Sienet MagicView 1100; Siemens, Erlangen, Germany) by three experienced radiologists (D.H.S., F.K., M.T.) without consultation and without knowledge of clinical, imaging, and histologic data. For lesion detection, interpreters independently analyzed images from all three phases during three sessions that were separated by intervals of at least 4 days. During the first session, only unenhanced images were assessed. During the second session, only corticomedullary-phase images were interpreted. During the third session, only nephrographic-phase images were analyzed. For lesion characterization, scans were interpreted during two sessions separated by intervals of at least 1 week. During the first session, combined unenhanced and corticomedullary-phase images were read, and during the second session combined unenhanced and nephrographic-phase images were analyzed. Problem cases were highlighted and reviewed together by using all scans. Judgments were reached by consensus when discrepancies were noted.

After the five sessions were completed, the series of images was presented randomly to the interpreters, who were also requested to assign a "lesion conspicuity score" according to a five-point scale in which 0 = not visible, 1 = barely visible, 2 = adequately visible, 3 = good visibility, 4 = excellent visibility. Lesion conspicuity scores were calculated by taking the average conspicuity score of the three observers for each lesion in the first, second, and third series, respectively. The radiologists were allowed to rate images only at 1.0-point gradations.

Cortical and medullary attenuation was measured in all patients on the same section as the lesion with use of circular region-of-interest cursors placed over the renal cortex and medulla to quantitate the differences in attenuation between these two portions of the kidney. The region-of-interest circle was kept constant in each patient for all renal measurements. The average of the measurements obtained by the three radiologists was calculated. Attenuation for the renal vein and inferior vena cava was measured on the unenhanced and the two contrast material–enhanced scans. The diameter of the region-of-interest circle used for measurements of attenuation of the renal vein and inferior vena cava (at the junction of the main renal veins) was maximized to the diameter of the vessel without including edges.

The size (< 8 mm, 8–15 mm, or 16–30 mm in maximum diameter), location (cortical or medullary), and attenuation (contrast enhancement and enhancement pattern) of each detected lesion were recorded for all scans. Differences in attenuation of the lesion and that of the kidney were calculated for each lesion by subtracting the average attenuation of the lesion from that of the surrounding renal cortex and medulla, respectively.

Cystic renal lesions were classified according to the Bosniak criteria into simple benign cysts (class I), minimally complicated cysts (class II), moderately complicated cysts (class III), and cystic carcinomas (class IV) (8,17). A diagnosis of angiomyolipoma was made when a lesion contained components with the attenuation of fat (> −10 HU). A lesion was considered an indeterminate mass if it had an attenuation of more than 20 HU and exhibited borderline or equivocal enhancement after administration of contrast material or if high standard deviations and partial volume artifacts affected the attenuation coefficients. Solid lesions with attenuation similar to that of other soft-tissue structures in the abdomen were classified according to their contrast enhancement and enhancement pattern (homogeneous or heterogeneous).

Statistical analyses were performed with commercially available software (StatView; Abacus Concepts, Berkeley, Calif). Primary statistical analysis of the pooled data was performed on the basis of the paired Student *t* test for mean differences in objective region-of-interest measurements among the three helical series. A number of paired Student *t* tests were performed to analyze (*a*) the mean difference in the numbers of lesions detected on all scans; (*b*) the mean difference between attenuation of the lesion and that of the cortex on all scans; (*c*) the mean difference between attenuation of the lesion and that

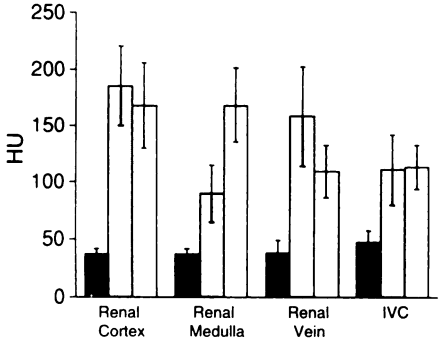

Figure 1. Bar graph compares the mean attenuation of the renal cortex, renal medulla, renal vein, and inferior vena cava on unenhanced (black bars), corticomedullary phase (gray bars), and nephrographic-phase (white bars) scans. Note the substantial difference in the attenuation of the renal medulla and that of the renal vein between corticomedullary-phase and nephrographic-phase scans. Error bars indicate standard deviations. *HU* = Hounsfield units, *IVC* = inferior vena cava.

of the medulla on all scans; and (*d*) the mean difference in lesion conspicuity score for all scans. A probability level of less than .01 indicated statistical significance. A confirmatory analysis was performed by using repeated calculations of analysis of variance (18). This method compares mean values for more than one group of the three helical series when measurements are taken at more than one point in time, which regulates differences among patients, differences among lesions in individual patients, and the relation between patients and helical scan sequences.

A Pearson correlation analysis was performed to assess differences between lesion attenuation and cortex attenuation as well as differences between the attenuation of the lesion and that of the medulla and to assess differences in the subjective lesion conspicuity scores. Two dichotomous variables were created to assess the relative differences in attenuation between the corticomedullary and nephrographic-phase scans. The first variable was separated into two groups. The first group included lesions with greater objective contrast on the nephrographic-phase scans; the second group included lesions with greater or equal contrast on the corticomedullary-phase scans. For the second variable (lesion conspicuity score), two groups were also characterized; the first group included lesions with greater conspicuity scores on the nephrographic-phase scans, and the second included those with greater or equal conspicuity scores on the corticomedullary-phase scans. Results were cross-tabulated, and the McNemar test was applied to the results to evaluate whether the proportion of lesions with greater contrast on the nephrographic-phase scans was similar to the proportion of lesions with higher conspicuity scores on the nephrographic-phase scans.

Table 1
Number of Renal Masses Detected in the Cortex and Medulla

Size of Lesion (mm)	Unenhanced Scans			Corticomedullary-Phase Scans			Nephrographic-Phase Scans		
	Cortex	Medulla	Total	Cortex	Medulla	Total	Cortex	Medulla	Total
<8	0	0	0	19	1	20	58	4	62
8–15	17	1	18	72	3	75	91	11	102
15–30	73	3	76	102	14	116	98	33	131
Total	90	4	94	193	18	211	247	48	295

RESULTS

A total of 279 scans in 93 patients constituted the final study group. In no case was image quality degraded secondary to motion artifact. There was no extravasation of contrast material or compromise of injection technique. The average attenuation (in Hounsfield units) and standard deviations of the renal cortex, renal medulla, renal vein, and inferior vena cava on all scans are shown in Figure 1.

Attenuation of the Renal Cortex and Renal Medulla

The average attenuation of the kidney on unenhanced images was 37 HU ± 5. Mean cortical attenuation was slightly but not statistically significantly greater on corticomedullary-phase scans than on nephrographic-phase scans. The average cortical attenuation on corticomedullary-phase scans was 185 HU ± 35, whereas the average attenuation on nephrographic-phase scans was 168 HU ± 33 ($P = .212$). Although average cortical attenuation was greater on the corticomedullary-phase scans, the difference in attenuation between the two scans was variable: An improvement in attenuation of at least 10 HU was attained in 74 of 93 cases (80%); however, attenuation on corticomedullary-phase scans was less than that on nephrographic-phase scans in 19 of 93 cases (20%). Average medullary attenuation was statistically significantly greater on nephrographic-phase scans (168 HU ± 33) compared with that on corticomedullary-phase scans (90 HU ± 25) in all cases ($P < .01$).

Attenuation of the Renal Vein and Inferior Vena Cava

Mean attenuation of the renal vein was 38 HU ± 11 before administration of contrast material. The relation between delay time and contrast material administration was statistically significant ($P < .01$). The average attenuation of the renal vein after a delay of 50 seconds (158 HU ± 44) was statistically significantly greater than that after a 180-second delay time (109 HU ± 23). Attenuation of the inferior vena cava was 47 HU ± 10 before administration of contrast material (Fig 1). The difference in average inferior vena cava attenuation between the two delay times (111 HU ± 31 vs 113 HU ± 19, respectively) was not statistically significant ($P = .0385$).

Lesion Detection and Lesion Characterization

A summary of size and location of the detected lesions is provided in Table 1. Overall, 94 lesions smaller than 3.0 cm were detected on unenhanced images. After administration of contrast material, the number of detected lesions increased statistically significantly ($P < .01$). On corticomedullary-phase scans, 211 lesions were depicted, and on nephrographic-phase scans 295 lesions were identified ($P < .01$) (Fig 2). Nine false-positive results were obtained. Six "medullary masses" were detected on corticomedullary-phase images but not on nephrographic-phase images and were attributed to misinterpretation of the renal medulla because of lack of medullary enhancement on corticomedullary-phase scans. In three cases, inhomogeneous enhancement of the renal medulla on corticomedullary-phase scans caused misidentification of the normal medulla as small renal lesions (Fig 3). Overall, the number of cortical lesions increased from 193 on corticomedullary-phase images to 247 on nephrographic-phase images (1.3 times), and the number of medullary lesions increased from 18 to 48 (5.3 times), respectively.

In the 93 patients studied, 211 lesions were seen on the corticomedullary-phase scans; there was a mean difference of 148 HU ± 54 between the attenuation of the lesion and that of the surrounding renal cortex and a difference of 50 HU ± 48 between attenuation of the lesion and that of the

surrounding renal medulla. On nephrographic-phase scans, 295 lesions were analyzed and the average difference between attenuation of the lesion and that of the surrounding renal cortex was slightly but not statistically significantly less (137 HU ± 44) than that for the corticomedullary phase. A statistically significant increase was noted in contrast enhancement of the lesion compared with that of the surrounding renal medulla (83 HU to 133 HU ± 44; $P < .01$) (Fig 4). Data on the characterization of small renal masses are summarized in Table 2.

Assessment of the relative conspicuity of lesions by the three radiologists (D.H.S., F.K., M.T.) was averaged for each lesion and was 0.9 ± 0.1 (barely visible) for the unenhanced scans, 2.6 ± 0.2 (adequate to good visibility) for the corticomedullary-phase scans, and 3.4 ± 0.1 (good to excellent visibility) for the nephrographic-phase scans ($P < .01$). The Pearson correlation analysis of the objective difference in contrast enhancement between the phases and the difference in conspicuity scores between the phases showed a correlation coefficient of .29, which was statistically significant ($P = .008$).

Objective measurements between the attenuation of the lesions and that of the surrounding renal cortex showed a greater difference with the shorter delay (50 seconds after contrast material administration) in 257 of 295 lesions (87%), while attenuation of the lesions and that of the surrounding renal medulla exhibited a greater difference with the longer delay (180 seconds after contrast material administration) in 289 of 295 lesions (98%) (Fig 5). In the cases with subjective visualization, 281 of 295 lesions (95%) were better or at least equally well seen during the nephrographic phase than during the corticomedullary phase of renal enhancement (Fig 6). Results of the McNemar χ^2 test of these proportions were not statistically significant ($P = .29$).

Twenty-eight patients underwent radical nephrectomy for RCC ($n = 25$), renal adenoma ($n = 1$), oncocytoma ($n = 1$), and renal tuberculoma ($n = 1$). Four patients underwent partial nephrectomy for RCC ($n = 1$) and moderately complicated cysts ($n = 3$). None of the lesions were smaller than 12 mm. Three masses were smaller than 16 mm in diameter: Two were RCC (12 and 15 mm, respectively), and one was a blood-containing cyst (14 mm). All other masses were 16–30 mm in maximum diameter. Figure 7 shows the differences between the attenuation of the lesion and that of the kidney for all RCCs during the three helical CT series.

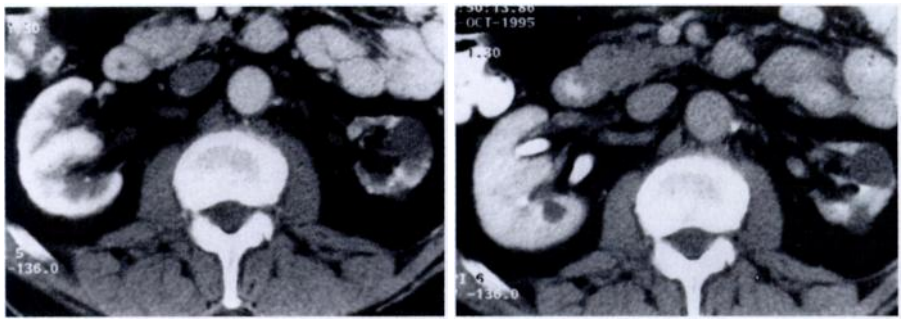

a. b.

Figure 2. CT scans obtained during the **(a)** corticomedullary phase and **(b)** nephrographic phase in a 69-year-old man with classes I and II renal cysts. In **a**, no renal mass was prospectively identified in the right kidney, but two cystic masses were seen in the small left kidney. This finding is related to atherosclerotic kidney disease. In **b**, a 1.1-cm cystic mass (14 HU) can be easily detected in the right kidney. Note also the better demarcation of both cystic masses in the left kidney due to homogeneous attenuation of the renal medulla and additional visualization of the collecting system.

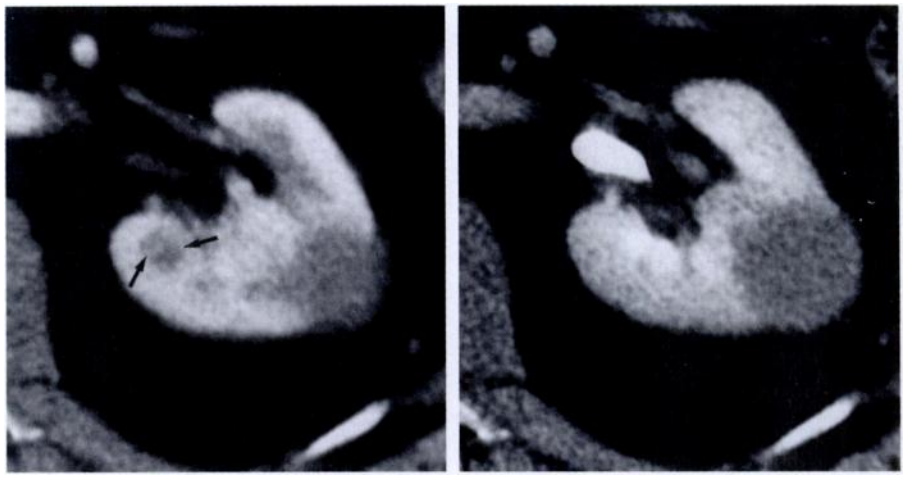

a. b.

Figure 3. CT scans obtained during the **(a)** corticomedullary phase and **(b)** nephrographic phase in a 59-year old man with RCC. **(a)** Scan demonstrates a solid mass. A second, smaller solid lesion (arrows) was also suspected in the posterior aspect of the middle of the right kidney. **(b)** Scan obtained at the same level shows better demarcation of the larger mass but homogeneous enhancement of the previously suspected lesion to the same extent as that of the renal medulla. The results of pathologic examination showed a single grade 1 clear cell RCC with a solid growth pattern.

DISCUSSION

Our findings can be summarized as follows: Nephrographic-phase scans provided greater lesion detection and improved lesion characterization of small renal masses than corticomedullary-phase scans. The capability to detect masses smaller than 3.0 cm was statistically significantly smaller on scans obtained during the corticomedullary phase than on those obtained during the nephrographic phase because of a substantially smaller difference between the attenuation of the lesion and that of the renal medulla. The difference in the detection rate was greater for smaller (< 1.5-cm) and medullary (5.3 times) masses than for larger (1.6–3.0-cm) and cortical (1.3 times) masses. The lack of medullary enhancement on corticomedullary-phase scans also resulted in potential pitfalls of image interpretation and false-positive results such as misidentification of an unenhanced renal medulla or of inhomogeneous medullary enhancement as a renal pseudotumor. The proportion of masses with greater differences in contrast enhancement during the corticomedullary phase was similar to the proportion of masses with greater conspicuity during the nephrographic phase.

A number of articles have been published that attest to the sensitivity of CT for the detection and diagnosis of small renal masses (2,4,19,20). In

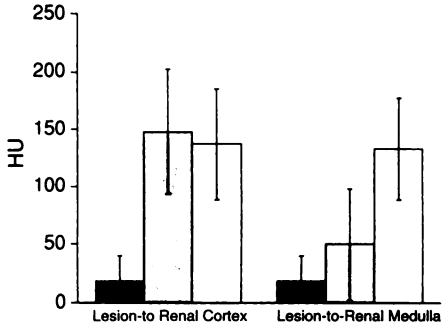

Figure 4. Bar graph demonstrates the mean difference between attenuation of the lesion and that of the renal cortex and attenuation of the lesion and that of the renal medulla on unenhanced (black bars), corticomedullary-phase (gray bars), and nephrographic-phase (white bars) scans. The difference between attenuation of the renal medulla and that of the lesion was statistically significantly greater during the nephrographic phase than during the corticomedullary phase ($P < .01$). Error bars indicate standard deviations. *HU* = Hounsfield units.

the era before CT, however, renal tumors smaller than 3.0 cm in diameter represented only 5% of all lesions (4). Hence, conventional contrast-enhanced CT has considerably improved detection and characterization of renal tumors and was widely accepted as the preferred method for evaluation of focal renal lesions before the introduction of helical CT (2,4,8,20,21).

Helical CT, however, provides many advantages over conventional CT in evaluation of the kidney. Helical scanning essentially minimizes data misregistration and partial volume averaging with use of a single breath-hold acquisition and allows for visualization of the entire kidney during several phases of contrast enhancement (9,15,16,22). The generated dataset is free from motion artifact and enables great flexibility in reconstructing images. These factors are of vital importance for the evaluation and characterization of small renal masses that otherwise may be missed (8,9,15,16,22).

Reports of experiences with helical CT scanning of the kidneys in patients with renal masses are just beginning to accumulate (15,16). In a review of helical CT literature, controversies regarding an optimal protocol for renal parenchymal imaging became evident. Although most investigators have favored images obtained during the cortical phase of renal enhancement (12–15), a few have evaluated renal masses with helical CT performed during a later phase of renal enhancement. Recently, Cohan et al (16) assessed renal masses on helical CT scans obtained during the corticomedullary and nephrographic phases of contrast enhancement. They concluded that CT scans obtained only during the corticomedullary phase of contrast enhancement failed to depict many renal masses that were easily seen on nephrographic images. Their findings are consistent with the findings in our study. Their study, however, was limited by a relatively small population group, the inclusion of only two solid masses, the lack of quantitative evaluation of kidney and lesion attenuation, and a marked temporal inhomogeneity in obtaining nephrographic-phase images. The temporal inhomogeneity of obtaining scans during the nephrographic phase of enhancement, as reflected by a mean standard deviation of 116 seconds, was attributed mainly to machine-related limitations (long tube cooling) and resulted in misinterpretation of five lesions on the nephrographic images. On the basis of their results, the authors suggested that the period immediately after acquisition of corticomedullary-phase images is not an optimal time to obtain nephrographic-phase images.

In our study, the longer and more precisely defined delay between the start of injection of contrast material and the acquisition of nephrographic-phase scans produced homogeneous enhancement of the kidney in all cases and often provided additional visualization of the collecting system. Fast-cooling, robust tubes allowed rapid tube cooling (approximately 10–20 seconds cooling time), which resulted in an exact onset of nephrographic phase scanning (mean standard deviation, 5 seconds). Also, the average of more than 12 lesions per patient detected by Cohan et al (16) implied that some patients had polycystic kidney disease rather than renal masses and might explain the difference in the number of medullary masses between their study and our findings.

The importance of and approach to the management of very small (< 15-mm) renal masses remains a diagnostic dilemma despite continuous refinements in CT scanner technology and imaging protocols. The increased detection of small renal masses also results in an increased detection of benign lesions and nonneoplastic masses, particularly cysts (7,8,20). To our knowledge, there are no data on this subject in the literature, and the way one handles these cases depends strongly on personal experience. We strictly followed the policy recommended by Bosniak (7,8). In younger or otherwise healthy individuals younger than 75 years of age who have small renal masses with attenuation clearly greater than 20–25 HU, sonography was performed to establish the diagnosis of a cyst and, if sonograms were not diagnostic, repeat CT scanning was performed 3 months later to determine enhancement of the lesion and to potentially initiate follow-up studies for assessment of possible tumor growth.

To our knowledge, this is the first study that involved the quantitative evaluation of the diagnostic potential of identically collimated helical CT scans at two different phases of renal enhancement in the detection and characterization of small renal masses. Most of the recent reports on assessment of renal masses, particularly cysts, have involved rescanning the kidneys in a conventional axial section after completion of helical CT scanning because tube cooling restrictions limited the available milliamperes. The acquisition of thin sections with overlapping reconstructions as well as the continuous use of 292 mA during the acquisition of unenhanced scans and during both phases of renal enhancement by means of a powerful generator and efficient detector system provided high accuracy of measurements and, hence, characterization of all renal masses that exceeded 15 mm in size and almost all masses (97 of 102 masses; 95%) 8–15 mm in maximum diameter. The high milliampere setting also may have increased the reliability of attenuation of renal masses smaller than 8 mm. Forty-six of 62 such lesions (74%) could be characterized. The relatively high number of class II cysts (55% on nephrographic-phase scans) identified in this group may not reflect the real rate of occurrence of class II cysts and can be attributed to partial volume averaging.

Small solid masses, however, may have the same attenuation as the incompletely enhanced medulla and, thus, similarly may be missed if additional nephrographic-phase scans through the kidneys are not obtained. The findings of our study demonstrate that images obtained during the nephrographic phase provided a statistically significantly greater difference between attenuation of small, solid RCCs and that of the renal medulla, which resulted in an increased conspicuity of such masses. Even in cases in which corticomedullary-phase scans were of equal value (ie, cystic RCC), the urologists (S.A., E.B.)

Table 2
Characteristics of Renal Masses in the Cortex and Medulla

Size of Lesion (mm)	Cystic Masses								Solid Masses		Indeterminate Masses	
	Class I		Class II		Class III		Class IV					
	CMP	NP	CMP	NP	CMP	NP	CMP	NP	CMP	NP	CMP	NP
<8	10 (50)	12 (19)	10 (50)	34 (55)	0	0	0	0	0	0	0	16 (26)
8–15	42 (56)	65 (61)	19 (25)	29 (31)	0	1 (1)	0	0	1 (1)	2 (2)	13 (17)	5 (5)
15–30	72 (62)	83 (64)	13 (11)	18 (14)	3 (3)	3 (2)	1 (1)	2 (2)	24 (21)	25 (19)	3 (3)	0
Total	124	160	42	81	3	4	1	2	25	27	16	21

Note.—Numbers in parentheses are the percentage of lesions seen during a given phase. CMP = corticomedullary phase, NP = nephrographic phase.

appreciated the more homogeneous display of the kidneys on nephrographic-phase scans, which subjectively improved their impression of an underlying pathologic condition.

Concordance between objective and subjective measurements that indicated that nephrographic-phase scans were better was noted in 247 of 295 lesions (84%). In 35 cases (12%), an objective measurement indicated that the contrast enhancement of both the kidney and the lesion during the corticomedullary phase was greater or equal to that during the nephrographic phase. Subjectively, these lesions were better seen on images obtained during the nephrographic phase. In nine cases (3%), there was concordance between the objective measurement and the subjective assessment, indicating the lesion was better displayed during the corticomedullary phase. In only four cases (1%) did lesions have a greater difference in attenuation from that of the surrounding kidney during the nephrographic phase but subjectively were better or equally well seen on the corticomedullary phase.

A review of these lesions suggested that the perceptual ability to detect lesions was dependent on more than just the difference between attenuation of the lesion and that of the surrounding kidney. Of the 32 small, solid masses detected, more than 26 masses (81%) were small RCCs. These results are similar to those of other studies that correlated CT images with pathologic findings (2,4). Similar to the results of Silverman et al (15), we have found that the typical helical CT appearance of small RCCs is that of a noncalcified mass with attenuation of 20 HU or more that enhances with contrast material. Some of the difficulties in the analysis of renal masses, however, are not solved with helical CT, particularly in solid benign lesions with imaging features indistinguishable from those of small RCCs.

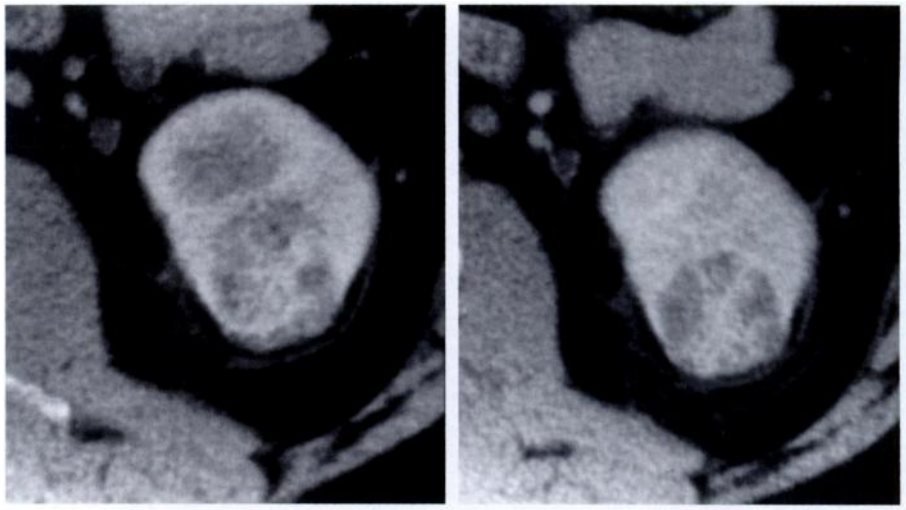

a. b.

Figure 5. CT scans obtained during the **(a)** corticomedullary phase and **(b)** nephrographic phase in a 56-year old man with RCC. **(a)** Scan demonstrates a 3.0-cm mass (38 HU) that enhanced heterogeneously to 83 HU. There is only fair demarcation of the mass from the inhomogeneously enhanced medulla. **(b)** Scan shows better demarcation and visualization of the mass. The results of pathologic examination revealed a grade 2 clear cell RCC with a solid growth pattern that contained many acellular regions and no areas of necrosis or deposits of hemosiderin.

Our study may have some limitations. First, the imaging protocol used would result in enormous film and related expenses; it also requires the use of a workstation. Since January 1995, however, our department has committed to working without hard-copy images. Although there were several problems initially, our preliminary experience with filmless radiology resulted in a substantial decrease in film and related expenses—a fact that has helped us to make the transition cost-effective. In addition, we have found that use of a picture archiving and communication system has improved efficiency. For instance, time savings have extended both to radiologists and to other hospital personnel. All images are now available electronically to all radiologists, and CT technologists are more productive because they no longer have to go through all the steps of producing and retrieving films. One disadvantage of soft-copy reading is that it can extend the workday by as much as 2 hours until the user becomes accustomed to the technology.

Another limitation of the study is that nephrographic phase scanning, although ideal for imaging the kidneys, is suboptimal for evaluation of the nearby organs, namely the liver and pancreas. The intention of this prospective study, however, was to assess the potential of dedicated renal parenchymal helical CT imaging performed before and during the corticomedullary and nephrographic phases of contrast enhancement for the detection and characterization of small renal masses. It is the policy in our department to perform specifically dedicated CT protocols for the evaluation of the abdominal organs.

In summary, our study quantitatively compared the diagnostic poten-

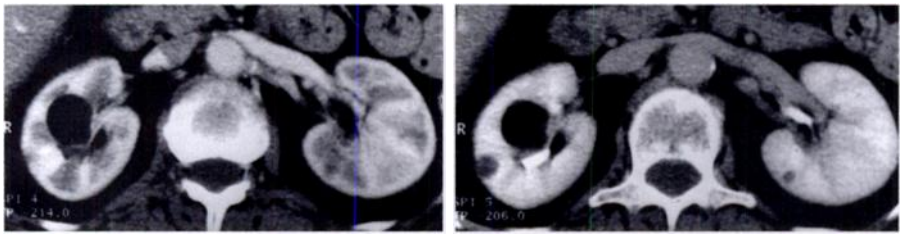

a. b.

Figure 6. Helical CT scans obtained during the **(a)** corticomedullary phase and **(b)** nephrographic phase in a 60-year-old woman with angiomyolipoma and two cysts. The images show a 2.5-cm mass in the central portion of the right kidney that predominantly contains fat with some soft-tissue areas (−67 HU). The contrast enhancement of both the cortex and the lesion was greater on **a** than on **b**, but the lesion was better seen subjectively on **b**. Note that two additional lesions are seen only on **b**: The 8-mm mass (attenuation, 17 HU) in the right kidney is a simple renal cyst, and the 4-mm mass in the left kidney is too small to characterize but probably represents a cyst.

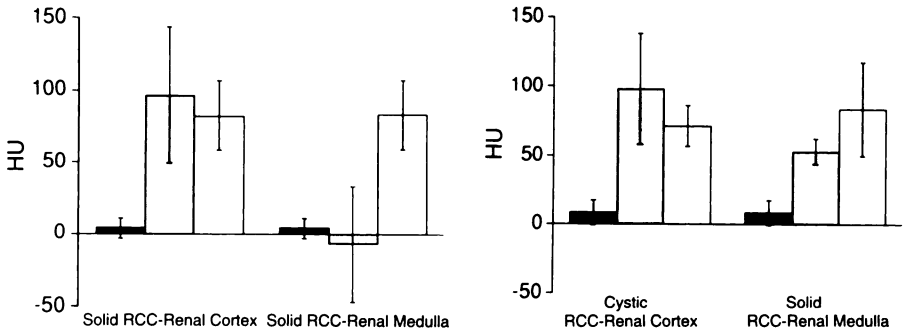

a. b.

Figure 7. Bar graph compares differences between attenuation of the lesion and that of the kidney for **(a)** 26 small solid RCCs, and **(b)** two cystic RCCs on unenhanced (black bars), corticomedullary-phase (gray bars), and nephrographic-phase (white bars) scans. The difference between attenuation of the renal medulla and that of the RCC during the nephrographic phase was statistically significantly greater than that during the corticomedullary phase ($P < .01$). Error bars indicate standard deviations. *HU* = Hounsfield units.

tial of identically collimated, thin-section helical CT performed during the corticomedullary and nephrographic phases of renal enhancement for the detection and characterization of small renal masses. The data demonstrate that nephrographic-phase scans allow greater detection, better visualization, and more accurate characterization of small renal masses than corticomedullary-phase scans. The use of only corticomedullary-phase scans poses the risk that renal masses will be missed or that an inhomogeneously enhanced renal medulla will be misdiagnosed as a renal mass. Although it is possible that corticomedullary-phase scans may not be necessary in the detection of small renal masses, we believe that additional experience is needed before corticomedullary-phase scans can be routinely eliminated. Corticomedullary-phase scans may be of value in patients with advanced renal cancer because of greater enhancement of renal veins and in those cases with "borderline" enhancement where multiple measurements are required to minimize the effect of scan artifacts and high standard deviations for final evaluation of the significance of the attenuation coefficients.

Despite the theoretic benefits of volumetric multiphasic CT, our findings indicate that some masses still remain indeterminate and require surgical removal for diagnosis. The combined use of high-quality helical CT scans (high milliampere settings) and a dedicated renal parenchymal imaging protocol at two different phases of contrast enhancement may decrease the need for surgery in patients with small or indeterminate renal masses identified with conventional or monophasic helical CT. Therefore, multiphasic helical CT currently seems to be the most effective method for evaluation of known or suspected small renal masses. A longer delay should be used when only monophasic scanning is used to detect and characterize small renal masses. ■

Acknowledgments: The authors thank Judith Heis, RT, and Renate Hutzl, RT, for technical assistance.

References

1. Thompson IM, Peek M. Improvement in survival of patients with renal cell carcinoma: the role of the serendipitously detected tumor. J Urol 1988; 140:487–490.
2. Curry NS, Schabel SI, Betsill WL. Small renal neoplasms: diagnostic imaging, pathologic features, and clinical course. Radiology 1986; 158:113–117.
3. Amendola MA, Bree RL, Pollack HM, et al. Small renal cell carcinomas: resolving a diagnostic dilemma. Radiology 1988; 166: 637–641.
4. Smith SJ, Bosniak MA, Megibow AJ, Hulnick DH, Horii SC, Raghavendra BN. Renal cell carcinoma: earlier discovery and increased detection. Radiology 1989; 170:699–703.
5. Butler BP, Novick AC, Miller DP, et al. Management of small unilateral renal cell carcinomas: radical versus nephron-sparing surgery. Urology 1995; 45:34–41.
6. Boring CC, Squires TS, Tong T, Montgomery S. Cancer statistics, 1994. CA Cancer J Clin 1994; 44:7–26.
7. Bosniak MA. The small (< 3.0 cm) renal parenchymal tumor: detection, diagnosis, and controversies. Radiology 1991; 179: 307–317.
8. Bosniak MA. Problematic renal masses. In: McClennan BL, ed. Syllabus: a categorical course in genitourinary radiology. Oak Brook, Ill: Radiological Society of North America, 1994; 183–191.
9. Kalender WA, Seissler W, Kotz E, Vock P. Spiral volumetric CT with single breath-hold technique, continuous transport, and continuous scanner rotation. Radiology 1990; 176:181–183.
10. Remy-Jardin M, Remy J, Giraud F, et al. Pulmonary nodules: detection with thick-section spiral CT versus conventional CT. Radiology 1993; 187:513–520.
11. Urban BA, Fishman EK, Kuhlman JE, Kawashima A, Hennessey JG, Siegelmann SS. Detection of focal hepatic lesions with spiral CT: comparison of 4-mm and 8-mm interscan spacing. AJR 1993; 160:783–785.
12. Zeman RK, Fox SH, Silverman PM, et al. Helical (spiral) CT of the abdomen. AJR 1993; 160:719–725.
13. Herts BR, Einstein DM, Paushter DM. Spiral CT of the abdomen: artifacts and potential pitfalls. AJR 1993; 161:1185–1190.
14. Heiken JP, Brink JA, Vannier MW. Spiral (helical) CT. Radiology 1993; 189:647–656.
15. Silverman SG, Lee BY, Seltzer SE, Bloom DA, Corless CL, Adams DF. Small (< 3 cm) renal masses: correlation of spiral CT features and pathologic findings. AJR 1994; 163:597–605.
16. Cohan RH, Sherman LS, Korobkin M, Bass JC, Francis IR. Renal masses: assessment of corticomedullary-phase and nephrographic-phase CT scans. Radiology 1995; 196:445–451.
17. Bosniak MA. The current radiological approach to renal cysts. Radiology 1986; 158: 1–10.
18. Dawson-Saunders B, Trapp RG. Basic and clinical biostatistics. 2nd ed. Norwalk, Conn: Appleton & Lange, 1994.
19. Levine E, Huntrakoon M, Wetzel LH. Small renal neoplasms: clinical, pathologic, and imaging features. AJR 1989; 153:69–73.
20. Curry NS. Small renal masses (lesions smaller than 3 cm): imaging evaluation and management. AJR 1995; 164:355–362.
21. Wills JS. Management of small renal neoplasms and angiomyolipoma: a growing problem. Radiology 1995; 197:583–586.
22. Rubin GD, Silverman SG. Helical (spiral) CT of the retroperitoneum. Radiol Clin North Am 1995; 33:903–932.